View metadata, citation and similar papers at core.ac.uk

brought to you by CORE

provided by Elsevier - Publisher Connector

Thin Solid Films 520 (2012) 4916–4920

Contents lists available at SciVerse ScienceDirect

Thin Solid Films

journal homepage: www.elsevier.com/locate/tsf

Hydrophobicity study of polytetrafluoroethylene nanocomposite films

Xianghui Hou, Peter T. Deem, Kwang-Leong Choy *

Faculty of Engineering, Energy and Sustainability Research Division, The University of Nottingham, Nottingham, NG7 2RD, United Kingdom

ARTICLE INFO

Article history:
Received 29 March 2011
Received in revised form 20 February 2012
Accepted 22 February 2012
Available online 3 March 2012

Keywords:
Hydrophobicity
Polytetrafluoroethylene
Inorganic fullerene-like tungsten disulfide
Water droplet
Oblate spheroid model
Roughness

ABSTRACT

In the present work, inorganic fullerene-like tungsten disulfide (IF-WS_2) nanoparticles have been incorporated into polytetrafluoroethylene films using aerosol-assisted deposition process. The hydrophobic behavior of the nanocomposite film has been investigated and the result shows that the hydrophobicity of PTFE films can significantly be improved with the incorporation of IF-WS_2 nanoparticles. An oblate spheroid model which takes into the consideration of surface roughness effect has been proposed, to simulate the hydrophobic behavior, based on the surface roughness and peak density of the nanocomposite films. This hydrophobic model can provide a useful guideline to describe and predict the hydrophobicity of nanocomposite films, from the input of parameters such as surface energy, roughness and liquid properties.

© 2012 Elsevier B.V. Open access under CC BY license.

1. Introduction

Polytetrafluoroethylene (PTFE) consisting of carbon and fluorine, is an excellent hydrophobic material for various applications [1]. The study of the hydrophobicity of PTFE and its related materials has been a popular topic within the last decade [2–5]. However, PTFE exhibits poor wear and abrasion resistance, which could lead to failure and leakage problems in its applications [6]. The incorporation of nanoparticles into PTFE-based matrices has been considered an effective way to increase the wear resistance and abrasion properties of PTFE for engineering applications. Various nanoparticles, such as nanodiamond [6], Zinc oxide (ZnO) [7], and alumina [8–10], have been incorporated into PTFE to form nanocomposites, especially in the forms of coatings or films, to increase the wear resistance and anti-abrasion properties. It is shown [10] that nanoparticles could be effective in reducing the wear, and preserving the low friction coefficient of PTFE. It is also reported that the incorporation of nanoparticles in PTFE matrix could improve the thermal stability and mechanical properties of the nanocomposites [6,11]. However, there is a lack of study on the hydrophobicity of the PTFE-based nanocomposites incorporating nanoparticles.

The incorporation of nanoparticles into PTFE matrix would significantly alter the surface morphology and chemical composition of the materials. The hydrophobic behavior of a solid surface is closely related to its micro/nanostructures as the hydrophobicity is governed by both the chemical composition and geometrical structure of the surface [12]. Currently, there are some modeling practices for water droplet, assuming the droplet is spherical [13,14], which does not take into account the gravity of droplet. Whyman et al. [15] proposed an oblate spheroid model and reported a more accurate description on droplet with the consideration of gravity. But the model mainly concentrated on the contact angle and base area, and the roughness effect of the surface was ignored.

In the present work, inorganic fullerene-like tungsten disulfide (IF-WS_2) nanoparticles have been incorporated into PTFE films using aerosol-assisted deposition process. IF-WS_2 nanoparticles have onion-like hollowed structure, which are suitable to be used as solid lubricants [16]. They have been incorporated in various nanocomposite films or coatings [17–19]. The main focus here is to investigate the hydrophobic behavior of the IF-WS_2/PTFE nanocomposite film. An oblate spheroid model which takes into the consideration of surface roughness effect has also been proposed, to simulate the hydrophobicity of the nanocomposite films.

2. Experimental details

Stainless steel plates (length = 25 mm, width = 15 mm) were selected as substrates. Prior to deposition, all substrates were degreased and cleaned in an ultrasonic bath with ethanol. IF-WS_2 nanoparticles ranging from 80 to 220 nm were supplied by NanoMaterials Ltd. The chemical solution was prepared by mixing IF-WS_2 nanoparticles with PTFE particles (200 nm, GBR Technology) in aqueous solution. The solid content of the dispersion was controlled at 0.01–2 wt.%.

The dispersions were then atomized to generate fine aerosol droplets with nitrogen as carrier gas. The droplets were subsequently directed towards a heated substrate where the deposition occurred.

* Corresponding author. Tel./fax: +44 115 95 14031.
E-mail address: kwang-leong.choy@nottingham.ac.uk (K.-L. Choy).

0040-6090 © 2012 Elsevier B.V. Open access under CC BY license.
doi:10.1016/j.tsf.2012.02.074

The deposition temperature was set at 300 °C. Post-heat treatment was carried out to obtain uniform solid film and enhance the interface strength between the film and substrate. The post treatment was performed in nitrogen gas, at 380 °C for 10 min. The film thickness was controlled at around 4 μm via adjusting deposition time.

The nanocomposite films were characterized using a combination of X-ray diffraction (XRD), X-ray photoelectron spectroscopy (XPS), scanning electron microscopy (SEM) and atomic force microscopy (AFM). A Siemens D500 X-ray diffractometer with Cu-Kα radiation was employed to detect the phase and crystallinity of the films. The measurement was operated in a step scan mode with a step of 0.01, in the range of 2θ = 10–80°, using 40 kV voltage and 25 mA current. The film surface was characterized by an X-ray photoelectron spectroscopy (VG Scientific ESCALAB Mark II), with non-monochromatic Al Kα X-ray at anode potential of 12 kV and filament emission current of 20 mA. A Philips XL30 scanning electron microscope was used to observe the surface morphology and cross-section of the films. The SEM operating voltage was 20 kV and the samples were pre-coated with gold layer to ensure good surface conductivity. Veeco CP-Research Scanning Probe Microscope was used under contact mode to measure the surface roughness of the films. The surface hydrophobicity of the films was determined by a FTÅ200 Dynamic Contact Angle System. Contact angles were calculated by fitting a mathematical expression to the shape of the water droplet and then calculating the slope of the tangent to the droplet at the liquid–solid–vapor interface.

3. Results and discussion

3.1. Microstructure of IF-WS_2/PTFE films

Fig. 1 shows phase and surface composition of the deposited films characterized by XRD and XPS. The content of IF-WS_2 nanoparticles is 10 wt.% in the nanocomposite film. In Fig. 1(a), both diffractions have a sharp (100) peak at 2θ of 18.1°, indicating that the molecular chains of PTFE are predominately parallel to the substrate surface [20]. There is a small peak at 2θ of 14.3° in the diffraction of the nanocomposite film, which is attributed to the (002) plane of IF-WS_2. It means that IF-WS_2 nanoparticles remain unchanged after the aerosol deposition and the post-heat treatment, and the incorporation of IF-WS_2 nanoparticles does not alter the crystallization of the PTFE matrix. Fig. 1(b) is XPS spectrum of PTFE nanocomposite film with 10 wt.% IF-WS_2. F and C are the major elements in the film, and small amount oxygen could also be detected, which is resulted from the surface adsorption of O_2 and CO_2. No obvious tungsten band peak can be detected, indicating that all IF-WS_2 are fully covered by PTFE matrix and there is no naked nanoparticle on the surface. Similar results are also observed from the nanocomposite films with higher loading of IF-WS_2. In additional, no nitrogen is found on the film surface from XPS analysis, confirming that nitrogen is not involved in the surface reaction during the heat treatment.

Fig. 2 shows SEM images of the nanocomposite film with 10 wt.% IF-WS_2. IF-WS_2 nanoparticles can be clearly observed from both the surface and the cross-section of the film. As compared to ceramic matrix based (Cr_2O_3) nanocomposite coatings [18], IF-WS_2 nanoparticles are less agglomerated and more evenly distributed inside the PTFE matrix. The results confirm that IF-WS_2/PTFE nanocomposite films have been produced.

The surface characteristic of the deposited films are also determined by AFM, as shown in Fig. 3. Root mean square (RMS) roughness of the films could be obtained from the AFM analysis. The RMS roughness of pure PTFE films is 112 nm, while the value increases to 192 nm on the surface of PTFE nanocomposite films with 10 wt.% IF-WS_2. The surface roughness of the films has increased significantly with the incorporation of IF-WS_2 nanoparticles, as seen in Fig. 4(a). The increase of roughness could be attributed to the possible agglomeration of nanoparticles and the higher viscosity of the nanocomposite film during the heat treatment. AFM data provides roughness statistics from both films, so that it would be used as a measure for the hydrophobic state.

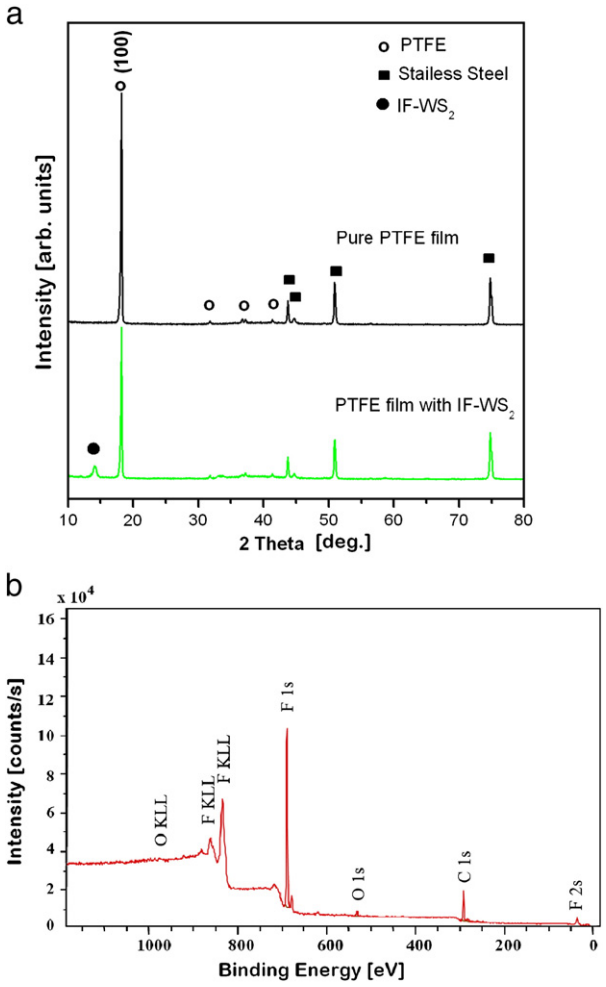

Fig. 1. Phase and surface composition of the deposited films: (a) XRD patterns of pure PTFE and IF-WS_2/PTFE films; (b) XPS spectrum of PTFE nanocomposite film with 10 wt.% IF-WS_2.

3.2. Hydrophobicity of the nanocomposite films

The hydrophobicity of the deposited films is determined by water contact angle measurement, as shown in Fig. 4. The obtained contact angle is the average value from 5 testing, with error normally within ±2°. The experimental results would aid the understanding of the thermodynamic behavior of nanocomposite films in contact with a liquid droplet. The pure PTFE film shows a water contact angle of 108°, which is similar to the reported value [2]. After the incorporation of IF-WS_2 nanoparticles, hydrophobic behavior of the PTFE film can be significantly improved, increasing the likelihood of a super hydrophobic state. With the increase of the IF-WS_2 content, the contact angle of the film increases, as shown in Fig. 4(a). As the AFM images show that the nanoparticle incorporation would drastically affect the roughness of the surface, a rougher surface structure is one of the key factors to lead to more hydrophobic behavior.

3.3. Modeling of hydrophobicity of the nanocomposite films

This study has focused on the mathematical modeling of a hydrophobic surface in contact with a liquid. It attempts to relate the chemical composition, surface roughness and contact angle for materials

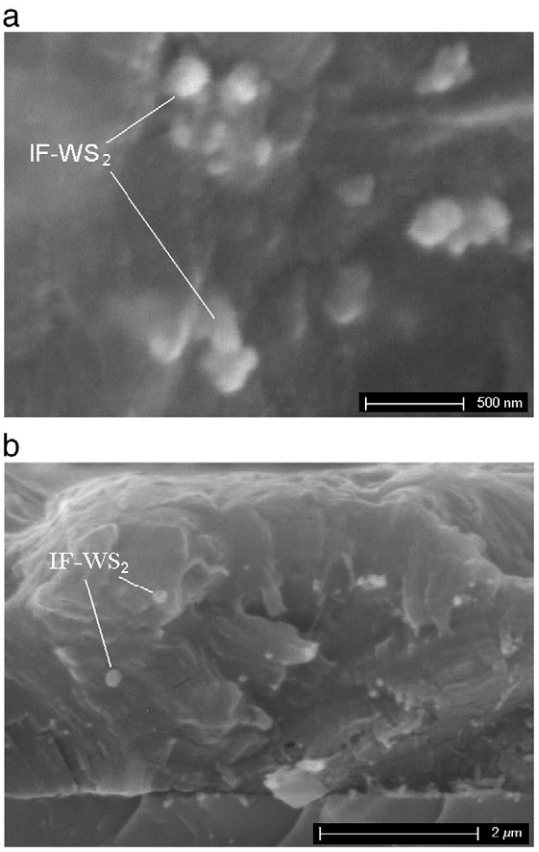

Fig. 2. SEM images of the IF-WS_2/PTFE films. (a) Surface morphology and (b) cross-section.

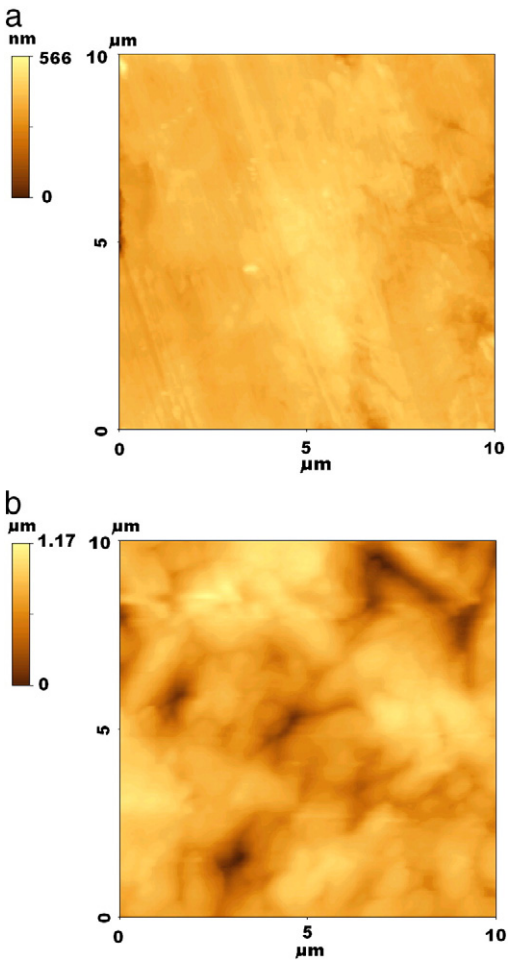

Fig. 3. AFM images of pure PTFE film (a) and PTFE nanocomposite film with 10 wt.% IF-WS_2 nanoparticles (b).

and water. In order to predict the probable contact angle of a water droplet on material surface, firstly, the geometry of the droplet needs to be established. The effects of both hydrophobicity and liquid characteristics have been initially taken as factors, thus allowing the model to be more flexible. An oblate spheroid is considered here, and its cross-section would give an ellipse (Fig. 5) with the characteristic Eq. (1).

$$\frac{(x-h)^2}{a^2}+\frac{(y-k)^2}{b^2}=1 \tag{1}$$

where a is the major radius, b is the minor radius, h and k are offsets. The equation considers two offsets, h and k. The x axis is considered to be the material surface, and the displacement k is related to the z factor which would be directly linked to the surface energy and roughness, as discussed later in this section. After replacing k with the Z value (a measure of hydrophobicity) as calculated later and re-arranging for x, we could obtain Eq. (2):

$$x=\sqrt{a^2}-\sqrt{\frac{a^2(y-b+z)^2}{b^2}} \tag{2}$$

The model relies on the "Z" function. This function contains information relating to both the hydrophobic state of the surface-liquid interface, and information on the surface chemistry itself in the form of surface energy. Using the geometry of the droplet, the surface topography and the surface chemistry of the material, it is possible to predict the interaction behavior of water repelling surface. The relation between the surface energy and "Z" factor can be described as follows: firstly, a droplet's aspect ratio and volume is characterized; then the Z value can be estimated based on empirical data for the surface energy. This estimation is then used to calculate the corresponding surface energy; iteration is then preformed to yield a more precise surface energy.

When determining the hydrophobic behavior of a solid liquid interface, there are three well defined hydrophobic states [21]: (a) Cassie state, where the deflection of the droplet is minimal as compared to the height of the surface roughness, forming an air pocket; (b) Wenzel state, where the surface peaks are well within the droplet, and no air pocket is formed; (c) Transitional state, which is between Cassie and Wenzel state. These three states determine the level of thermodynamic involvement of any material at the interface. The effect of surface roughness on the wetting behavior of surfaces is well described in theory. However, very little of this theory has been applied in realistic environments. In order to incorporate the engineering roughness as a measure for this hydrophobic state, it has been non-dimensionalized by calculating the maximum deflection of a liquid surface under the pressure of an average surface peak. The schematic diagram of droplet deflection and the importance of peak density are shown in Fig. 6, based on the calculation of the maximum deflection of a liquid droplet surface supported by average surface peaks. Where Mg is the weight of the droplet, n is the estimated number of peaks supporting the droplet, T is the surface tension of the droplet, D is the defection of the droplet, and H is the average height of the surface peaks. The ratio of this deflection versus the engineering roughness provides a good estimation for hydrophobic state. A high ratio suggests a Wenzel state and a very low ratio effectively suggests a Cassie state, with that in between suggesting a transitional state. Ultimately these states reduce the effective contact area. A reduced contact area can easily be approximated as a proportional reduction in surface energy.

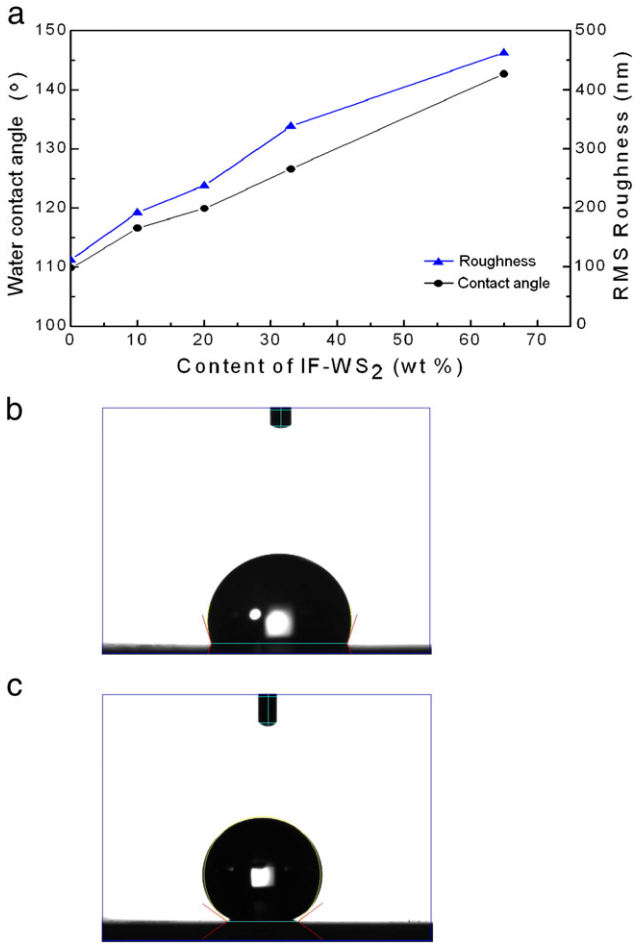

Fig. 4. Water contact angle and surface roughness of the deposited films: (a) water contact angle and surface roughness versus content of IF-WS_2 in the nanocomposite films; (b) water droplet on pure PTFE film, contact angle θ = 108.0°; (c) water droplet on IF-WS_2/PTFE nanocomposite film (65 wt.% IF-WS_2), contact angle θ = 142.7°.

By analyzing the surface profile it is possible to estimate the number of peaks for a given surface area. Subsequently, with this mechanics it is possible to compute the 2-D deflection under a load at the surface. For this particular pair of surface and droplet, it is then possible to determine the hydrophobic state. If the deflection is greater than the roughness there will be zero reduction in area and Wenzel state should be considered. If the deflection is considerably smaller than the roughness, Cassie state is true. Finally, for comparable roughness and deflection a transitional state needs be considered.

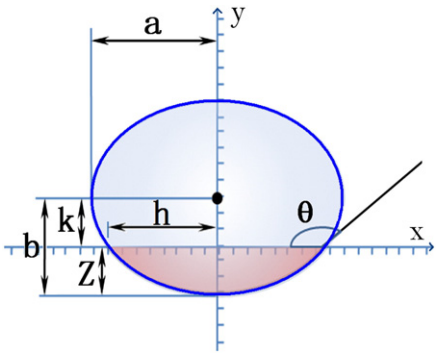

Fig. 5. Ellipse model of water droplet on material surface.

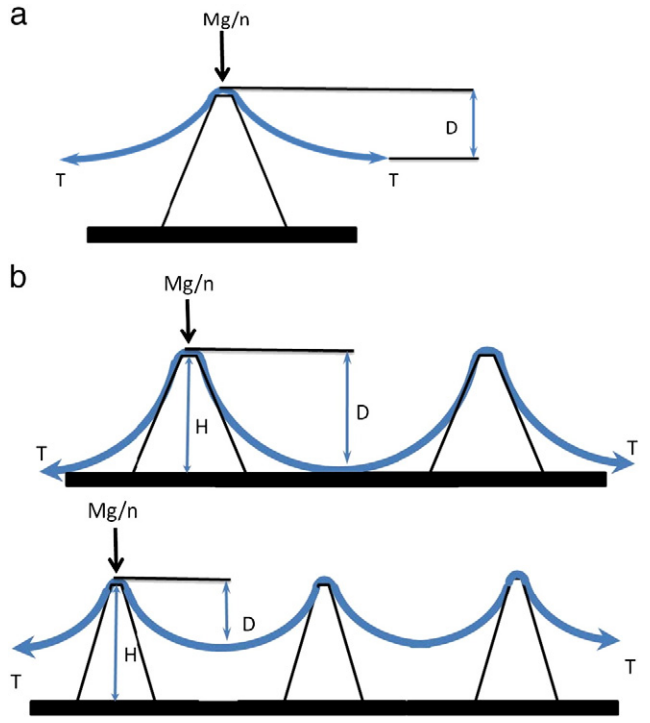

Fig. 6. Schematic diagram of droplet deflection on surface peaks. (a) Droplet deflection on a surface peak; (b) importance of peak density when considering drop deflection.

The flow chart of the modeling is shown in Fig. 7. In order to realize the numeral modeling, the following assumptions have been made:

(i) The surface tension of a water droplet is considered constant, and the water droplet of constant volume can be approximated as an oblate spheroid of aspect ratio 0.9, which is estimated from the experimental work.
(ii) The surface is treated as series of *n* uniformly distributed peaks with a height equal to the roughness of the surface.
(iii) The contact area between droplet and surface is considered proportional to the droplet deflection/peak height.

The initial input data requires the liquid surface tension and surface energy for the equivalent smooth surface. The system calculates "*Z*" factor for the interaction, which leads to an iterative loop. At this point, information is required on the surface topography and roughness, specifically the number of peaks for a known sample area and the surface roughness. This information, along with the *Z* factor, is then entered into an iterative loop; initially the *Z* factor is used to

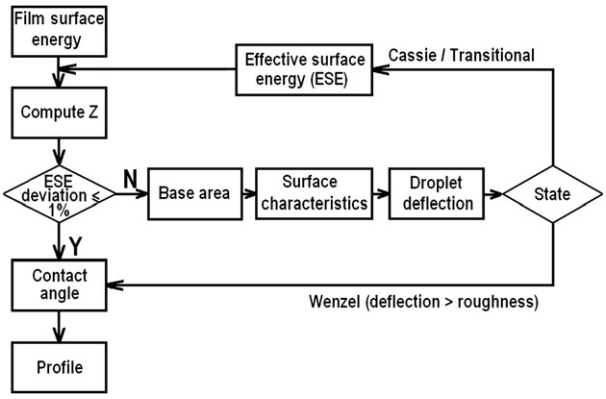

Fig. 7. Flow chart of the modeling program.

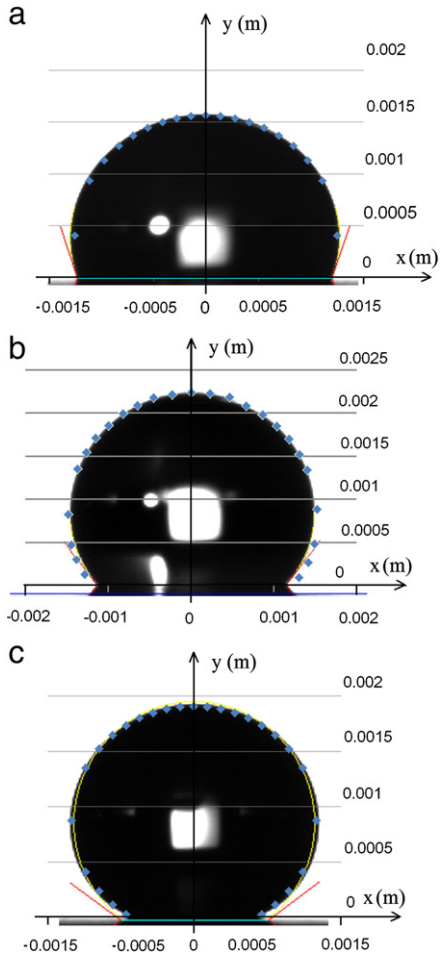

Fig. 8. Superimposed calculated profiles of water droplet on PTFE films: (a) Pure PTFE film with 0 wt.% IF-WS_2, calculated contact angle 104°; (b) nanocomposite film with 33 wt.% IF-WS_2, calculated contact angle 126.4°; and (c) nanocomposite film with 65 wt.% IF-WS_2, calculated contact angle 146.2°.

calculate the base area. This information is then used to determine the hydrophobic state. If Wenzel state is true, the contact angle for the associated specific *Z* factor is the output contact angle for the system. If the state is Cassie or transitional, the original surface energy is replaced with an effective surface energy, and a new *Z* function is calculated corresponding to the new base area and the iteration is continued. The loop is broken when the deviation of effective surface energy falls within 1% of the previous iteration. At this point both the contact angle and *Z* function are outputs, the program then calculates the droplet profile.

Examples of the modeling results are shown in Fig. 8. The black droplets are the real experimental photos on different surfaces and the circular profiles consisting of small squares are the calculated results. Both the droplets and modeling profiles are described in meter-scale (m) in Fig. 8. The experimentally measured contact angles of PTFE nanocomposite films with 0, 33 wt.% and 65 wt.% IF-WS_2 are 108.0°, 126.6°, and 142.7°, respectively. While the calculated contact angles are 104° for pure PTFE film, 126.4° for film with 33 wt.% IF-WS_2, and 146.2° for film with 65 wt.% IF-WS_2, respectively. The result shows that the model could give good description on surface hydrophobic contact. It demonstrates a useful attempt to quantitatively link the surface hydrophobic contact with materials properties and surface roughness.

4. Conclusions

It has been demonstrated that the incorporation of IF-WS_2 nanoparticles can improve the hydrophobic behavior of the PTFE film significantly, increasing the likelihood of a super hydrophobic state. With the increase of the IF-WS_2 content, the contact angle of the films also increases. Since the roughness of PTFE films increases significantly with the incorporation of IF-WS_2 nanoparticles, it is believed that the rougher surface structure would lead to more hydrophobic behavior.

An oblate spheroid droplet model based on the surface roughness and peak density has been proposed to study the hydrophobic behavior of IF-WS_2/PTFE nanocomposite films, with the consideration of different hydrophobic states. The model relies on the "*Z*" function, which contains information relating to the hydrophobic state of the surface–liquid interface, and information on the surface chemistry itself in the form of surface energy. It demonstrates a useful attempt to quantitatively link the surface hydrophobic contact with materials properties and surface roughness.

Acknowledgements

The authors would like to acknowledge the financial supports provided by EU and EPSRC, under FP6 Foremost and Follow-on-Fund project EP/G006113/1, respectively. We also would like to thank Mr. Martin Roe for performing XPS surface analysis and NanoMaterials Ltd for kindly supplying IF-WS_2 nanoparticles for this research.

References

[1] S. Veeramasuneni, J. Drelich, J.D. Miller, G. Yamauchi, Prog. Org. Coat. 31 (1997) 265.
[2] J. Zhang, J. Li, Y. Han, Macromol. Rapid Commun. 25 (2004) 1105.
[3] M. Krasowska, J. Zawala, K. Malysa, Adv. Colloid Interface Sci. 147 (148) (2009) 155.
[4] Y. Chen, Z. Zhao, J. Dai, Y. Liu, Appl. Surf. Sci. 254 (2007) 464.
[5] M. Doms, H. Feindt, W.J. Kuipers, D. Shewtanasoontorn, A.S. Matar, S. Brinkhues, R.H. Welton, J. Mueller, J. Micromech. Microeng. 18 (2008) 055030.
[6] J.Y. Lee, D.S. Lim, Surf. Coat. Technol. 188 (189) (2004) 534.
[7] F. Li, K. Hu, J. Li, B. Zhao, Wear 249 (2002) 877.
[8] W.G. Sawyer, K.D. Freudenberg, P. Bhimaraj, L.S. Schadler, Wear 254 (2003) 573.
[9] D.L. Burris, S. Zhao, R. Duncan, J. Lowitz, S.S. Perry, L.S. Schadler, W.G. Sawyer, Wear 267 (2009) 653.
[10] D.L. Burris, B. Boesl, G.R. Bourne, W.G. Sawyer, Macromol. Mater. Eng. 292 (2007) 387.
[11] H.Y. Wang, X. Feng, Y.J. Shi, X.H. Lu, J. Rare Earth 25 (2007) 40.
[12] H. Sun, M. Luo, W. Weng, K. Cheng, P. Du, G. Shen, G. Han, Nanotechnology 19 (2008) 125603.
[13] A. Dupuis, J.M. Yeomans, Langmuir 21 (2005) 2624.
[14] J.T. Hirvi, T.A. Pakkanen, J. Chem. Phys. 125 (2006) 144712.
[15] G. Whyman, E. Bormashenko, J. Colloid Interface Sci. 331 (2009) 174.
[16] L. Rapoport, N. Fleischer, R. Tenne, Adv. Mater. 15 (2003) 651.
[17] X.H. Hou, C.X. Shan, Surf. Coat. Technol. 202 (2008) 2287.
[18] X.H. Hou, K.L. Choy, Thin Solid Films 516 (2008) 8620.
[19] W.X. Chen, J.P. Tu, Z.D. Xu, R. Tenne, R. Rosenstveig, W.L. Chen, H.Y. Gan, Adv. Eng. Mater. 4 (2002) 686.
[20] S.T. Li, E. Arenholz, J. Heitz, D. Bkerle, Appl. Surf. Sci. 125 (1998) 17.
[21] X.J. Feng, L. Jiang, Adv. Mater. 18 (2006) 3063.